

Random measurement errors in LuSci

A. Tokovinin

Version 2. February 12, 2008 [errcalc.tex]

1 Introduction

Turbulence profile in a surface layer can be measured by a lunar Scintillometer, LuSci (also called lunar SHABAR) [1, 3]. The profile is reconstructed from the covariances of signals from several detectors located in appropriate spatial pattern. The covariances are measured with certain statistical errors related to the properties of the scintillation signals. In this note we estimate the errors and calculate their effect on the restored turbulence profile.

2 Formulas for errors of covariances

A lunar scintillometer measures fluctuations of the lunar flux caused by turbulence. The covariance of the normalized intensity fluctuations from two sensors separated by a baseline b , $C(b)$, is computed from the measured intensities I_i and I_j (at detectors i and j) as

$$C_{ij}(\mathbf{b}_{ij}) = \frac{\langle \Delta I_i \Delta I_j \rangle}{\langle I_i \rangle \langle I_j \rangle} = \langle x_i x_j \rangle, \quad (1)$$

where $x_i = \Delta I_i / \langle I_i \rangle$ are normalized intensity fluctuations. The statistical averaging is done on a finite data sample of duration T , so the measured quantities C_{ij} are estimates of the true covariances which we denote by the same symbols (God forgive). The baseline vector is \mathbf{b}_{ij} . The normalized variance (scintillation index) $\sigma^2 = C_{ii}$ is a specific case of coincident detectors and zero baseline. The intensity fluctuations x_i have zero mean by definition and are Gaussian random variables.

Textbooks give formulas for calculating the variances of statistical estimates. For example, Eq. 8.95 of Bendat & Piersol [2] reads

$$\text{Var}[C_{ij}] = \frac{1}{T} \int_{-T}^T \left(1 - \frac{|\zeta|}{T}\right) [C_{ii}(\zeta)C_{jj}(\zeta) + C_{ij}(\zeta)C_{ji}(\zeta)] d\zeta, \quad (2)$$

where $C_{ij}(\zeta)$ is the temporal covariance of the signals. In the following we assume that the averaging time T is much larger than the signal correlation time. The auto-covariances C_{ii} and C_{jj} are, of course, equal, while $C_{ji}(\zeta) = C_{ij}(-\zeta)$. This simplifies Eq. 2 to

$$\text{Var}[C_{ij}] = \frac{1}{T} \int_{-\infty}^{\infty} [C_{ii}^2(\zeta) + C_{ij}(\zeta)C_{ij}(-\zeta)] d\zeta. \quad (3)$$

Now if we define the time constant τ_{ij} ,

$$\tau_{ij}(\mathbf{b}_{ij}) = \sigma^{-4} \int_{-\infty}^{\infty} [C_{ii}^2(\zeta) + C_{ij}(\zeta)C_{ij}(-\zeta)] d\zeta, \quad (4)$$

the expression for the error variance becomes

$$\text{Var}[C_{ij}] = \sigma^4 \tau_{ij}/T. \quad (5)$$

These time constants depend on the baselines. The time constant for zero baseline $\tau_0 = \tau_{ii}$ is a useful characteristic of the signal variation in one detector. The approximation (3) is valid for $T \gg \tau_0$. The relative error of the variance measurement is equal to $\sqrt{\tau_0/T}$.

For calculating the error of the reconstructed profile, we also need to know the correlation between different covariance estimates. Some covariances involve common detectors and are obviously correlated. Moreover, the scintillation signal contains an important low-frequency component, therefore *all* covariance estimates, even with different detector pairs, are correlated.

Let $A = C_{ij}$ and $B = C_{kl}$ be two measured covariances, where some indices may coincide. The signals $x_i = \Delta I_i/I_i$ are Gaussian, so the fourth moment is expressed by a combination of the second moments,

$$\langle AB \rangle = \langle x_i x_j x_k x_l \rangle = \langle x_i x_j \rangle \langle x_k x_l \rangle + \langle x_i x_k \rangle \langle x_j x_l \rangle + \langle x_i x_l \rangle \langle x_j x_k \rangle. \quad (6)$$

The correlation (we do not say covariance to avoid confusion of terminology) between two errors is

$$\text{Cov}(AB) = E(\Delta A \Delta B) = E(AB) - E(A)E(B) = \langle x_i x_k \rangle \langle x_j x_l \rangle + \langle x_i x_l \rangle \langle x_j x_k \rangle. \quad (7)$$

Continuing the analogy with Bendat & Piersol, the estimates obtained over a finite time $T \gg \tau_0$ will have the error correlation expressed as

$$\text{Cov}[AB] = \frac{1}{T} \int_{-\infty}^{\infty} [C_{ik}(\zeta)C_{jl}(\zeta) + C_{il}(\zeta)C_{jk}(\zeta)] d\zeta. \quad (8)$$

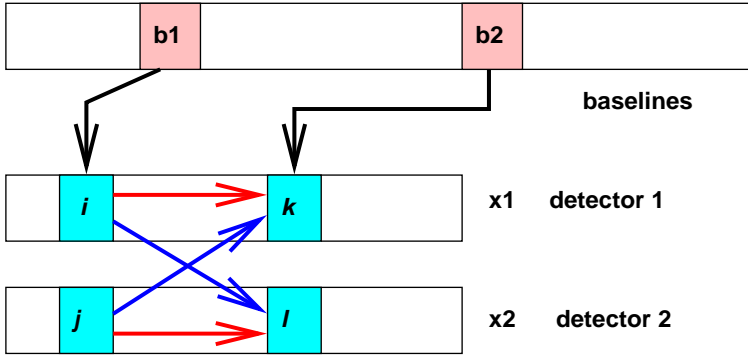


Figure 1: To the calculation of the error correlation (see text). [base-order.fig]

The formula (8) shows that the correlation of errors of covariances measured at two baselines b_1 and b_2 depends on the covariances at some other baselines. Figure 1 illustrates the calculation. Let the first baseline involve signals x_i and x_j , the second – signals x_k and x_l (some indices may coincide). The first term of (8) is a product of covariances between the first and second pairs of signals, as illustrated by the two large red horizontal arrows. The second term involves two combinations of the type “first with second” shown by the inclined blue arrows. The order of the signals in each combination does matter because $C_{ij}(\zeta) = C_{ji}(-\zeta)$. In the case of two coincident baselines $i = k$, $j = l$, (8) is transformed into (3).

3 Estimation of the temporal covariance for one layer

In order to proceed with the calculation, we need to estimate the temporal covariance $C_{ij}(\zeta)$. The scintillation signal from different layers is independent, so the covariances are just sums over all layers weighted by the turbulence integrals $C_n^2 dz$ in each layer. We start with one layer and use the Taylor hypothesis, supposing that the layer moves as a whole with the wind speed vector \mathbf{V} . Then the temporal covariance is related to the spatial covariance in the obvious way,

$$C_{ij}(\mathbf{b}_{ij}, \zeta) = C_{ij}(\mathbf{b}_{ij} + \zeta \mathbf{V}, 0). \quad (9)$$

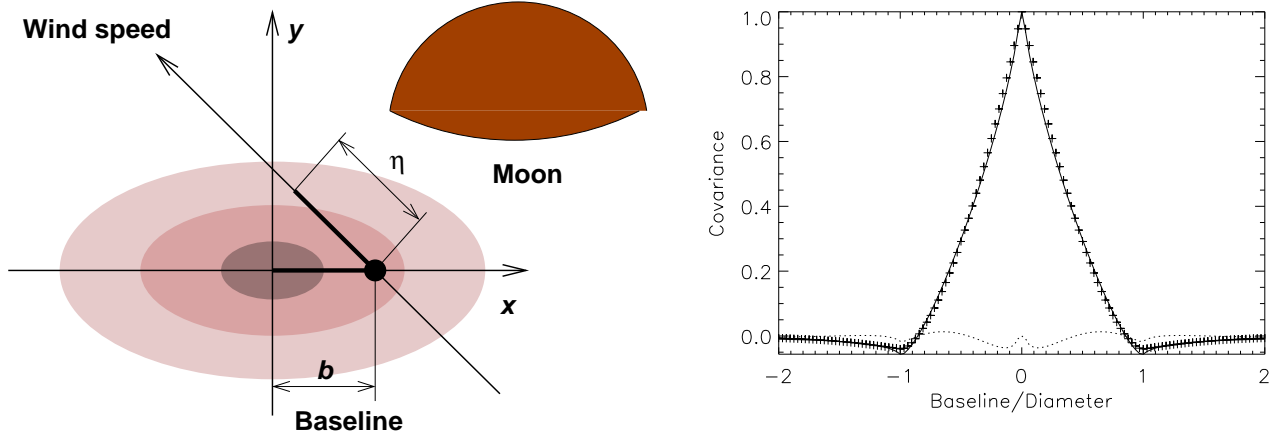


Figure 2: Left: The relation between temporal and spatial covariances of lunar scintillation (see text). Right: the covariance in normalized coordinates (full line) and its model (crosses). The difference between them is plotted in dotted line. [tempcov.fig,acfmod.ps]

Figure 2 helps to visualize this relation. The two-dimensional spatial covariance of scintillation resembles a cone centered at the coordinate origin and falling below zero at baseline $d = \theta z$ – the projected diameter of the Moon at a distance z from the detector. The covariance is circularly symmetric for the full Moon, but has elliptical contours otherwise, being more extended along the terminator line. The right-hand plot shows a cut through the center of this function, normalized to one at the origin. If the baseline \mathbf{b}_{ij} is not zero, the temporal covariance $C_{ij}(\zeta)$ equals the spatial covariance along the line passing through the baseline point and parallel to the wind vector, with the displacement along the line being $\eta = V\zeta$. The result depends on the baseline length and orientation with respect to the terminator, lunar phase, the speed and direction of the wind. This large number of variables make the modeling very difficult, so some approximations must be made.

If we neglect both the scintillation averaging by the detector and the finite turbulence outer scale, all covariances will have the same shape, they are only stretched spatially in proportion to $d = \theta z$ (projected lunar diameter) and scaled in amplitude. The covariance function normalized to one at the origin is a universal function $C'(b')$ of the normalized distance $b' = b/(\theta z)$. The analytical expression for this function is given by Hickson & Lanzetta [1]. For the purpose of numerical calculation, we use

the following approximation:

$$C'(b') \approx \begin{cases} 1.06[1 - |b'|^{1.6}] - 0.06/[1 + 0.5(b')^4] & \text{for } |b'| < 1 \\ -0.06/[1 + 0.5(b')^4] & \text{for } |b'| \geq 1 \end{cases} \quad (10)$$

This formula is over-plotted in Fig. 2 with crosses. Its maximum deviations from the exact curve are -0.037 and $+0.013$ – much less than the errors caused by the un-modeled surface structure of the Moon, for example.

We suppose that the baseline is oriented along the terminator (parallel to the coordinate axis x) – a good approximation for LuSci with its baseline along declination, especially near full Moon. The dependence on the wind speed V can be eliminated by replacing the temporal coordinate ζ with the spatial one $\eta = \zeta V$. The only two remaining variables are the relative baseline length b/d and the angle α between the wind and the baseline. A general expression for the normalized temporal covariance is then

$$C_{ij}(b', \eta') = C'(b'_x + \eta' \cos \alpha, b'_y + \eta' \sin \alpha), \quad (11)$$

where the normalized coordinates are $b' = b/d$ and $\eta' = \eta/d$.

For one detector, the calculation of the time constant leads to $\tau_0 = 0.86 \theta z/V$. The time constants at non-zero baselines decrease approximately as $\exp[-(b'/0.3)^2]$. However, modeling of the time constant for one layer is of little value because the combined time constants are calculated from the products of covariances (cf. Eq. 8) and hence depend on the turbulence profile in non-linear way. In other words, the errors of the measured covariances *depend on the scintillation produced by all layers jointly*. Scintillation from high layers is slow and will dominate the measurement errors, even if we are interested only in measuring the low-altitude turbulence with LuSci.

4 Estimation of the reconstruction errors

Now all elements are in place to evaluate the errors of the reconstructed turbulence profiles. We recall that the linear restoration method used in LuSci [4] consists in defining a certain number K of “layers”. The turbulence integrals J_k are derived from the linear combinations of the measured covariances,

$$J_k = \sum_l R_{kl} C_l = \int C_n^2(z) \mathcal{R}_k(z) dz. \quad (12)$$

Here we numbered all L baselines with the index l . The restoration matrix R has dimensions $K \times L$. Each line of this matrix corresponds to a restored layer with a certain response function $\mathcal{R}_k(z)$

$$\mathcal{R}_k(z) = \sum_l R_{kl} W_l(z) \quad (13)$$

being a linear combination of the weighting functions $W_l(z)$. Examples of such response functions are given in Fig. 3.

We compare here two scintillometer arrays. The first, L-1, has four 1-cm square detectors in a linear configuration with coordinates (0, 10, 13.5, 38) cm. This array has been used already in several missions. An optimized set of response functions $\mathcal{R}(z)$ peaking at the distances z of (3, 12, 40,

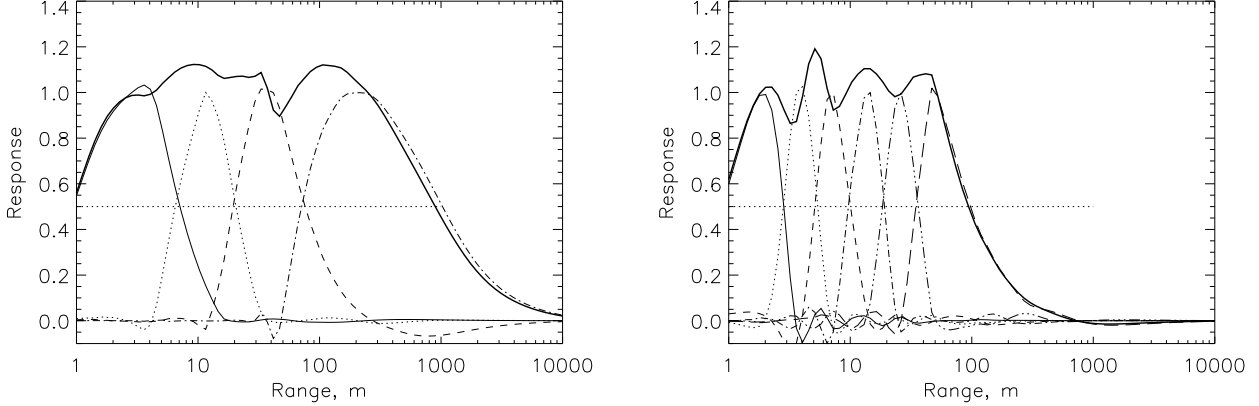


Figure 3: The response functions $\mathcal{R}_k(z)$ for the scintillometer arrays L-1 with 4 detectors (left) and L-2 with 6 detectors (right). The sum of all responses is over-plotted as thick line. [allwf_l1.ps,allwf_l2.ps]

200) m has been used for profile reconstruction, with a total number of baselines $L = 7$ (six pairwise combinations plus the zero baseline).

The second array, L-2, contains 6 detectors in the linear arrangement with coordinates (0, 12, 15, 17, 21, 40) cm giving $L = 16$ non-redundant baselines. The weighting functions corresponding to these baselines and full Moon are plotted in Fig. 4. A set of 6 response functions peaking at distances (2, 3.8, 7.5, 14, 25, 50) m is also displayed in Fig. 3. The method of deriving these functions was modified to enforce their zero value at $z > 500$ m. The increased number of detectors and baselines permits to reach a better altitude resolution $\Delta z/z \sim 2$ (at FWHM level). In comparison, $\Delta z/z \sim 4$ for L-1 (cf. Fig. 3).

We can calculate the covariance matrix of the measurements S_C using Eq. 8 and then derive the covariance matrix of the profile errors S_J in the usual way,

$$S_J = R S_C R^T. \quad (14)$$

The diagonal elements of the matrix S_J are equal to the variances of the profile estimates σ_{Jk}^2 . The *signal-to-noise* ratio can be defined as $r_k = J_k/\sigma_{Jk}$. If the turbulence profile $C_n^2(z)$ is scaled without changing its shape, the time constants and signal-to-noise ratios do not change.

In the spirit of Tokovinin & Travouillon [5], we use a two-exponent model of the turbulence profile

$$C_n^2(z) = A \exp(-z/h_0) + B \exp(-z/h_1) \quad (15)$$

with $A = 5 \cdot 10^{-15} \text{ m}^{-2/3}$, $B = 10^{-16} \text{ m}^{-2/3}$, $h_0 = 30$ m, and $h_1 = 10$ km. The logarithmic altitude grid with 80 layers from 1 m to 10 km is defined. The sampling of this grid $z_{i+1}/z_i = 1.12365$ is small enough to capture the details of the weighting and response functions. The turbulence integrals in each layer J_i equal the products of the $C_n^2(z_i)$ defined by the model (15) with the step Δz_i . The covariances equal $C_l = \sum_i W_l(z_i) J_i$. The scintillation index in one detector $\sigma^2 = 7.75 \cdot 10^{-8}$. The total turbulence integral of our model $J = Ah_0 + Bh_1$ corresponds to the seeing $\varepsilon = (J/6.8 \cdot 10^{-13})^{0.6} = 1.37''$. The

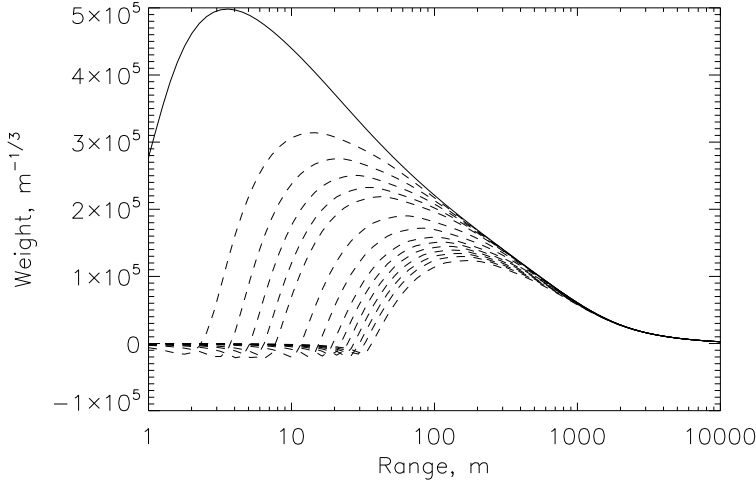


Figure 4: Weighting functions $W_l(Z)$ for the L-2 scintillometer array with 6 detectors. [wt.l2.ps]

ground-layer seeing calculated from the sum of J_k depends on the response functions. For L-1, the GL seeing $\varepsilon = 0.61''$ is larger than for L-2, $\varepsilon = 0.42''$, for this reason.

We suppose that the wind speed in the whole atmosphere increases from 1 m/s at the ground to 20 m/s at 1 km, then stays constant. An alternative case with a constant $V = 5$ m/s in all layers was tried as well. Our calculation assumes the averaging time $T = 20$ s corresponding to the effective averaging length $VT = 100$ m for $V = 5$ m/s. The results can be easily applied to other wind speed and averaging time values by noting the proportionality $\sigma_{Jk} \propto (VT)^{-1/2}$ which follows from the relations given above.

The calculations are performed by the code `moonx3.pro` containing several sub-programs. The code is suitable for both for L-1 and L-2. First, we run `prepare` to calculate the weights, then `allwf` to define the response functions, and, finally, `tempcov` to determine the temporal covariances and errors.

In the calculation of the temporal covariances, we adopt the time sampling of 5 ms and a grid size of ± 256 points, or time lags up to ± 1.28 s. For each layer, the shape of $C_l(\zeta)$ is determined by the simple model (10) and (11) multiplied by $W_0(z_i)J_i$, i.e. normalized by the signal variance at zero baseline. Thus, we neglect the influence of the finite detector size and turbulence outer scale on the shape of $C_l(\zeta)$, but account for these effects in the normalization. This is a good approximation at altitudes from 10 m to 100 m.

When the wind speed is parallel to the baseline, all functions $C_l(\zeta)$ have the same shape, being only shifted by b_l/V from the coordinate origin. This is not realistic, so we adopt the wind direction at 45° to the baseline. Figure 5 (left) shows the set of temporal covariances for the L-1 array resulting from the combined effect of all layers. The wide “wings” of all functions are determined by the high-altitude turbulence and are essentially the same for all baselines. For comparison, we show in the same figure the experimentally measured temporal covariance. Its wings are artificially shortened by using short individual accumulation time (5 s) and some high-pass filtering in the calculation of the covariance.

The table below gives the matrix of the correlation times τ_{lk} (in milliseconds) for the L-1 array and our model. The baselines (in cm) are listed in the first line. We see that $\tau_0 = 138$ ms. The calculation

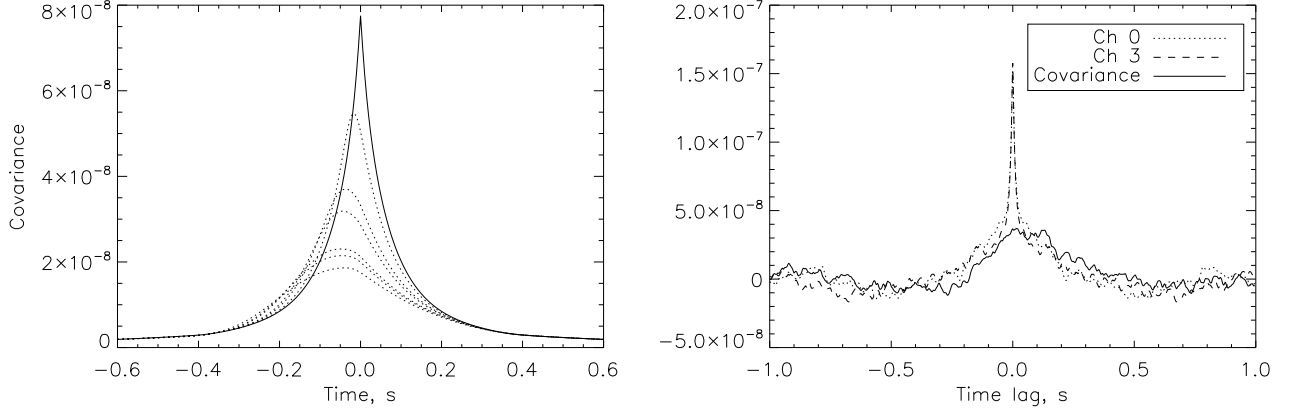


Figure 5: Temporal covariance functions. Left: our model for the L-1 array (zero baseline in full line, other baselines in dotted lines). Right: covariance at baseline 38 cm (full line) and at zero baseline (in two detectors) measured on February 5, 2007 at 7:45 UT at Cerro Tololo with $T = 20$ s. [tempcov_l1.ps,cov0745_03.ps]

follows the prescription (8). The array of temporal covariances at all baselines is used as the input. Then, for each pair of baselines, we select the two lines of this array corresponding to the first term of (8), revert the temporal argument where necessary, and sum the product of these lines, approximating the integral over ζ . The second term is calculated in the same way.

0.0	3.5	10.0	13.5	24.5	28.0	38.0
137.8	70.6	96.9	87.6	46.0	49.3	59.9
70.6	125.3	89.5	89.9	66.5	66.6	54.2
96.9	89.5	107.3	96.5	53.9	57.3	58.0
87.6	89.9	96.5	101.5	56.7	57.1	58.0
46.0	66.5	53.9	56.7	91.2	82.6	63.2
49.3	66.6	57.3	57.1	82.6	89.4	67.1
59.9	54.2	58.0	58.0	63.2	67.1	85.9

We see that all time constants τ_{lk} take similar values, i.e. the errors of covariance measurements are strongly correlated, as expected. We have established that a single turbulent layer at altitude z leads to a time constant $\tau_0 = 0.86 \theta z / V$. The above model with constant wind speed $V = 5$ m/s gives $\tau_0 = 112$ ms; in this case, the combined effect of all layers can be likened to a single layer at $z \approx 75$ m.

At the final step, we multiply the matrix of time constants by σ^4 / T to get the error covariances S_C and use (14) to calculate the errors of the results J_K . For the L-1 array, we obtain the signal-to-noise ratio $S/N = (2.1, 2.1, 1.9, 3.7)$ in the four restored layers. Thus, all integrals are measured with a relative statistical error of $\sim 50\%$ which can be reduced to 25% by increasing the integration time to $T = 80$ s. The noise will be less on the nights with higher wind speed.

Under the same conditions, the L-2 array has $S/N = (0.3, 0.6, 0.8, 0.7, 1.0, 1.2)$. The restored turbulence profile is noisier for two reasons. First, the measurement errors of J_k are slightly larger

because the restoration operation is more complex. Secondly, the J_k themselves are smaller because the “layers” are thinner owing to the better altitude resolution of L-2. The results are gathered in the Table below, with integrals J_k in the units of $10^{-13} \text{ m}^{1/3}$. The calculations were repeated with different parameters of the turbulence profile. For example, with a 10-fold increase of A (strong ground-layer turbulence), the S/N in the first layer improves. These numbers are marked S/N* in the Table. Slightly higher S/N are obtained with a constant wind speed of 5 m/s. Yet another case with the standard turbulence model and a faster wind $V = 3 + 0.0025 z$ (this approximates the median wind profile at Cerro Pachón) leads to $\tau_0 = 127 \text{ ms}$ and $\text{S/N} = (3.1, 3.0, 2.5, 3.4)$ for the L-1 array.

	L-1 array (4 detectors)				L-2 array (6 detectors)					
z0, m	3	12	40	200	2	3.8	7.5	14	25	50
J_k	0.32	0.49	0.60	1.57	0.08	0.12	0.21	0.31	0.40	0.46
S/N	2.1	2.1	1.9	3.7	0.3	0.6	0.8	0.7	1.0	1.2
S/N*	2.7	2.6	2.8	1.4	0.4	0.7	1.0	1.0	1.2	1.3

5 Conclusions

The lunar scintillation signal contains a slowly varying component originating at high altitudes and correlated between all detectors. The covariances between signals in a scintillometer array estimated from a sample of finite duration T have substantial statistical errors. These errors should not be confused with the detector noise, they are caused by the statistical nature of the signal itself. The effect of these errors was evaluated numerically using a representative model of the turbulence profile. It is shown that by increasing the number of the detectors in the array, we can improve the altitude resolution, at a cost of reduced measurement precision. Therefore, a longer integration time will be necessary to compensate for this loss. For example, the S/N for 5-min. integrations and L-2 array will reach 4.

References

- [1] Hickson, P. & Lanzetta, K. 2004, PASP, 116, 1143
- [2] Bendat, J.S. & Piersol, A.G. Random Data. Analysis and measurement procedures. 1986, Wiley & Sons: New York.
- [3] Socas-Navarro, H., Beckers, J., Brandt, P. et al. 2005, PASP, 117, 1296
- [4] Tokovinin A. Restoration of turbulence profile from lunar scintillation. Unpublished report, January 23, 2007.
- [5] Tokovinin A., Travouillon T. 2006, MNRAS, 365, 1235